Metallurgy and Foundry Engineering – Vol. 40, 2014, No. 1, pp. 15–32
http://dx.doi.org/10.7494/mafe.2014.40.1.15

Ewa Rudnik, Przemysław Biskup

Electrochemical behavior of tellurium in acidic nitrate solutions

Elektrochemiczne zachowanie się telluru w kwaśnych roztworach azotanowych

Abstract

Electrochemistry of tellurium stationary electrode was studied in acidic nitrate solutions with pH 1.5–3.0. Cyclic voltammetry indicated that two products were formed at potentials above 300 mV (SCE): soluble $HTeO_2^+$ (500 mV) and sparingly soluble H_2TeO_3 (650 mV), but the former seemed to be an intermediate product for TeO_2 precipitation on the electrode surface. Formation of the solid products as porous layers was almost undisturbed and no electrode passivation was observed. H_2TeO_3 and TeO_2 dissolved to $HTeO_2^+$ under acidic electrolyte, but this process was hindered by pH increase. Cathodic polarization of tellurium electrode below –800 mV was accompanied by the evolution of H_2Te, which was then oxidized at the potentials approx. –700 mV. H_2Te generated in the electrochemical reaction decomposed to elemental tellurium as black powdery precipitates in the bulk of the solution and a bright film drifting on the electrolyte surface.

Key words: tellurium, cyclic voltammetry, pH, electrochemistry, nitrate

Streszczenie

Przeprowadzono badania elektrochemiczne telluru w kwaśnych roztworach azotanowych o pH 1.5–3.0. Pomiary metodą woltammetrii cyklicznej wykazały obecność dwóch produktów tworzących się przy potencjałach powyżej 300 mV (NEK): rozpuszczalny $HTeO_2^+$ (500 mV) i trudno rozpuszczalny H_2TeO_3 (650 mV), przy czym pierwszy z nich stanowi produkt pośredni tworzenia się TeO_2. Formowanie się produktów stałych w postaci porowatych warstw nie prowadziło do pasywacji elektrody. H_2TeO_3 i TeO_2 ulegały rozpuszczaniu pod wpływem roztworu z utworzeniem $HTeO_2^+$, lecz proces ten ulegał zahamowaniu przez wzrost pH. Katodowa polaryzacja

Ewa Rudnik Ph.D.: AGH University of Science and Technology, Faculty of Non-Ferrous Metals, Krakow, Poland; **Przemysław Biskup M.Sc.:** Royal Group, PO Box 5151, Eastern Ring Road, Abu Dhabi, United Arab Emirates; erudnik@agh.edu.pl

elektrody tellurowej poniżej –800 mV prowadziła do tworzenia się H_2Te, który ulegał utlenianiu przy potencjałach ok. –700 mV. H_2Te generowany w reakcji elektrodowej ulegał rozpadowi do telluru elementarnego występującego w dwóch postaciach (jako czarny osad i srebrzysty film).

Słowa kluczowe: tellur, woltamperometria cykliczna, pH, elektrochemia, azotan

1. Introduction

The fundamental electrochemistry of tellurium in acidic and alkaline aqueous solutions has been presented in some extent in general reviews [1, 2]. Most of the studies have been focused on the electrodeposition of tellurium from acidic solutions [3–9]. Recently, interest in this area has been renewed due to the electrochemical deposition of semiconductors such as CdTe [7], ZnTe [10] or Bi_2Te_3 [11, 12] as examples. These papers include usually additional experimental data on tellurium behavior. However, there is relatively limited information on the effect of the solution pH on the anodic oxidation of tellurium [13, 14]. Awad [13] determined potentials of tellurium anodes in acids ($HClO_4$, H_2SO_4, HNO_3) as a function of acid concentration and current density. He found that the type of the dissolution product depends on the pH range: $HTeO_2^+$ forms in the pH range of 0–0.8, H_2TeO_3 forms above pH 1.8, whereas both species are present at intermediate pH. In more concentrated solutions (pH below 0) tellurium dissolves to Te^{4+} ion.

More extended data were presented by Jayasekera et al. [14], who investigated tellurium electrode in a wide pH range (0–14). However, some doubts appear if H_2TeO_3 is considered as a product, since there are no cogent arguments for separate H_2TeO_3 molecule existence. It forms rather hydrated oxide, $TeO_2 \cdot xH_2O$.

The electrochemical behavior of tellurium is usually consistent with the predictions from E-pH diagram [15]. It is worth noting that various interpretations of electrode reactions detected during voltammetric studies were proposed. Cyclic voltammetric (CV) curves registered in acidic Te(IV) solutions in the potential range from –800 to 1000 mV (vs. NHE) reveal usually two anodic and three cathodic peaks. Attribution of appropriate electrochemical processes to the individual peaks is dependent on the electrolyte and substrate material (e.g. glassy carbon, gold, platinum, tellurium) due to the possibility of tellurium underpotential deposition.

In some cases there is no accordance in the mechanism of the reaction. For example, the cathodic peak at the potential from –400 to 500 mV (vs. NHE) is correlated with H_2Te evolution accompanied by metallic tellurium deposition. Martin-Gonzales et al. [11] reported that electrochemical reduction of $HTeO_2^+$ to H_2Te was followed by the precipitation of elemental tellurium in secondary chemical reactions. Wen et al. [12] suggested that the electrochemical reduction of tellurium metal to H_2Te was accompanied by secondary electrochemical reactions between H_2Te and $HTeO_2^+$. Some discrepancy in the literature data on the anodic process at the potential of approx. 800 mV (NHE)

was also found. A double peak appears sometimes at this potential. It was proposed that oxidation of bulk tellurium Te deposited overpotentially was accompanied by the dissolution of the metal deposited in the secondary electrochemical [12] or chemical reaction [6] as well as in the underpotential process [10].

Most of the CV studies were performed at one pH value and at one scan rate using acidic electrolytes containing tellurium(IV) species. There have been not more detailed studies on the behavior of bulk material. Moreover, no detailed identification of products of electrode reactions was reported. Hence, the aim of this work was to give further insights into the electrochemical processes of the polycrystalline tellurium investigated in nitrate solutions. Cyclic voltammetry in solutions with pH in the range of 1.5–3.0 is discussed.

2. Experimental

Electrochemical behavior of tellurium was studied in HNO_3 solutions in the pH range of 1.5–3.0. Tellurium electrodes were prepared from polycrystalline tellurium pieces (99.9%) embedded in duracryl resin leaving one active surface. The surface active area of each electrode was approx. 1 cm^2. Prior to each experiment tellurium samples were polished with diamond slurry (with the grain gradation of 3 μm and 1 μm). The electrodes were then thoroughly rinsed in deionized water and acetone (each stage was carried out in a laboratory ultrasonic cleaner for 10 min). The stationary tellurium electrodes in non agitated baths (100 cm^3) were used. Each measurement was carried out with a fresh tellurium surface and a fresh portion of the electrolyte. Platinum plate (6 cm^2) was used as the counter electrode. The reference electrode was saturated calomel electrode (SCE) and all potentials are reported against this electrode. Electrochemical measurements (principally cyclic voltammetry) were made using a potentiostat Atlas Sollich 98 EII. Potentials of the working electrode were ranging from –1800 mV to 1300 mV (SCE) to cover all reactions of interest in the investigated system. The potential range was scanned in both positive-going and negative-going sweeps with various scan rates (1–100 mV/s). For a detailed analysis, CV scans were registered in narrower potential ranges at a scan rate of 10 mV/s. A potentiostatic dissolution of tellurium was also carried out. Before and after potentiostatic measurement the electrode surface was observed by means of optical and scanning electron microscopes. Solid products of tellurium anodic oxidation were analyzed with SEM-EDS (Hitachi S 4700), whereas the concentration of the tellurium species soluble in the electrolyte was determined by means of ICP method (Perkin Elmer ICP AES "Plasma 40"). Additional voltammetric measurements in acidic nitrate solutions saturated with TeO_2 were performed on a glassy carbon electrode. All experiments were performed at room temperature and repeated a few times to check the reproducibility of the results.

3. Results and discussion

3.1. General voltammetry

Cyclic voltammograms for stationary tellurium electrode were registered in nitrate solutions of various pH from the range from 1.5 to 3.0 and at various sweep rates. Figure 1 shows the influence of pH on the course of the voltammetric curves registered in a wide potential range (from –1800 to 1300 mV vs SCE). Independently on the direction of the forward scan similar results were obtained. Therefore, cyclic voltammograms with the positive-going initial scans are only presented in Figure 1 and discussed below.

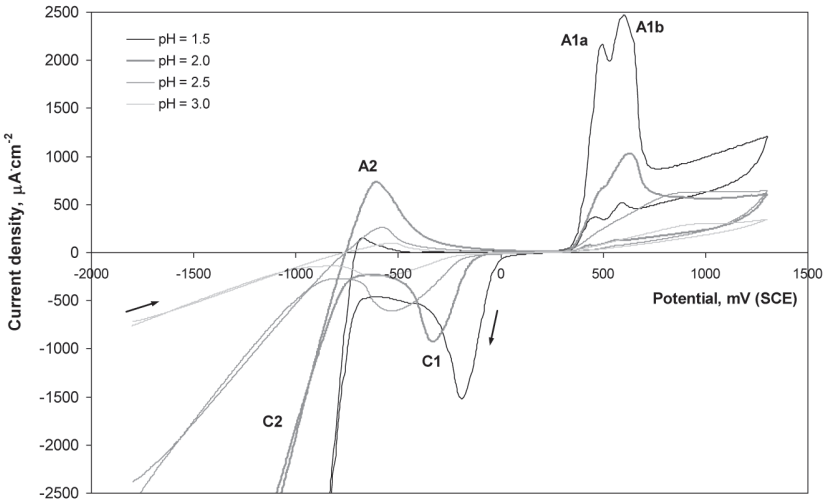

Fig. 1. Cyclic voltammograms for Te in HNO_3 solutions of various pH. Scan rate: 10 mV/s; starting potential: –1800 mV (SCE); sweeps initiated towards positive potentials; switching reversal potential: 1300 mV(SCE)

Three anodic peaks and two cathodic responses were found in the CV plots. The potential scan started at –1800 mV and was going to more positive values. Initially, it was accompanied by the flow of the cathodic current (C2), but above from –740 to –710 mV the anodic peak (A2) appeared. At potentials from approx. –330 mV to approx. 300 mV a low anodic current density region was observed. The anodic current increased again above 330–350 mV giving a double peak (A1). The last one degenerated gradually into one wide peak when pH of the electrolyte was increased from 1.5 to 3.0.

In the backward sweep, the cathodic peak (C1) was observed in the potential range below 0 mV. Further decrease in the potential lead to the cathodic current flow (C2) with the negative-going curves overlapped previous positive-going sections of the voltam-

mograms. As the solution pH was increased both anodic peaks A1a and A1b became lower in heights, turned gradually into one wide peak with a maximum slightly shifted towards more positive potentials. The cathodic peak C1 was also reduced; it grew wider and displaced to more negative potentials, simultaneously. The cathodic currents in the C2 region decreased seriously from approx. 30 mA/cm^2 at pH = 1.5 to approx. 0.75 mA/cm^2 at pH = 3.0 at the final potential of –1800 mV. The anodic peak A2 enlarged with the pH change from 1.5 to 2.0, but further increase in the pH was accompanied by the reduction and slight shifting of the peak maximum towards more positive potentials.

The CV curves showed that an increase in the solution pH inhibited gradually both anodic processes occurring at potentials above 330 mV and both cathodic reactions, whereas the effect of pH on the anodic process at potential approx. –700 mV was more complicated. All electrochemical processes are discussed further in details. Correlations between individual peaks were found in additional CV measurements. They were performed in various potential ranges for each pH. However, for clarity the results for two extreme pH values are only described.

3.2. Anodic polarization

Figure 2 shows typical CV curves registered in narrow potential ranges at pH of 1.5 and 3.0 with the potential sweeps commenced in the negative direction. Similar measurements were performed in the same potential ranges with the positive-going forward scans and no differences in the CV plots were found. When a potential sweep was realized between –700 mV and 500 mV (Fig. 2 a, b), the increase in the anodic current above 350–400 mV (A1a) was accompanied by the cathodic peak (C1a) at the potentials of range from –350 to –400 mV. If the anodic range was extended to 800 mV at pH 1.5, two oxidation peaks (A1a and A1b) gave two cathodic peaks (C1a and C1b) in the negative-going sweep (Fig. 2c). It shows that both reduction peaks C1a (approx. –400 mV) and C1b (approx. –200 mV) are correlated with the oxidation peaks A1a (480–520 mV) and A1b (600–650 mV), respectively.

It is interesting that two cathodic peaks (C1a at –430 mV and C1b at –320 mV) were recorded at pH 3.0 (Fig. 2d), despite the absence of two coalescing anodic peaks above 350 mV. A further increase in the potential range up to 1300 mV revealed again two anodic peaks (A1a, A1b) at pH 1.5 and one anodic peak (A1 at 780 mV) at pH 3.0, but only a wide cathodic peak C1 (Fig. 2e, f) in the negative-going step was found. The latter shifted from approx. –200 mV to approx. –480 mV with the pH change from 1.5 to 3.0. However, it should be noted that a weak bend of the curve corresponding to the peak C1a occurred at pH 1.5. Neither C1a nor C1b reduction peaks were observed if sweeping was performed from the starting potentials less than 300 mV towards more negative values (Fig. 2 g, h). It shows that the cathodic peaks (C1a, C1b) were due to the reduction of two products of tellurium oxidation at potentials above 300 mV (A1a, A1b).

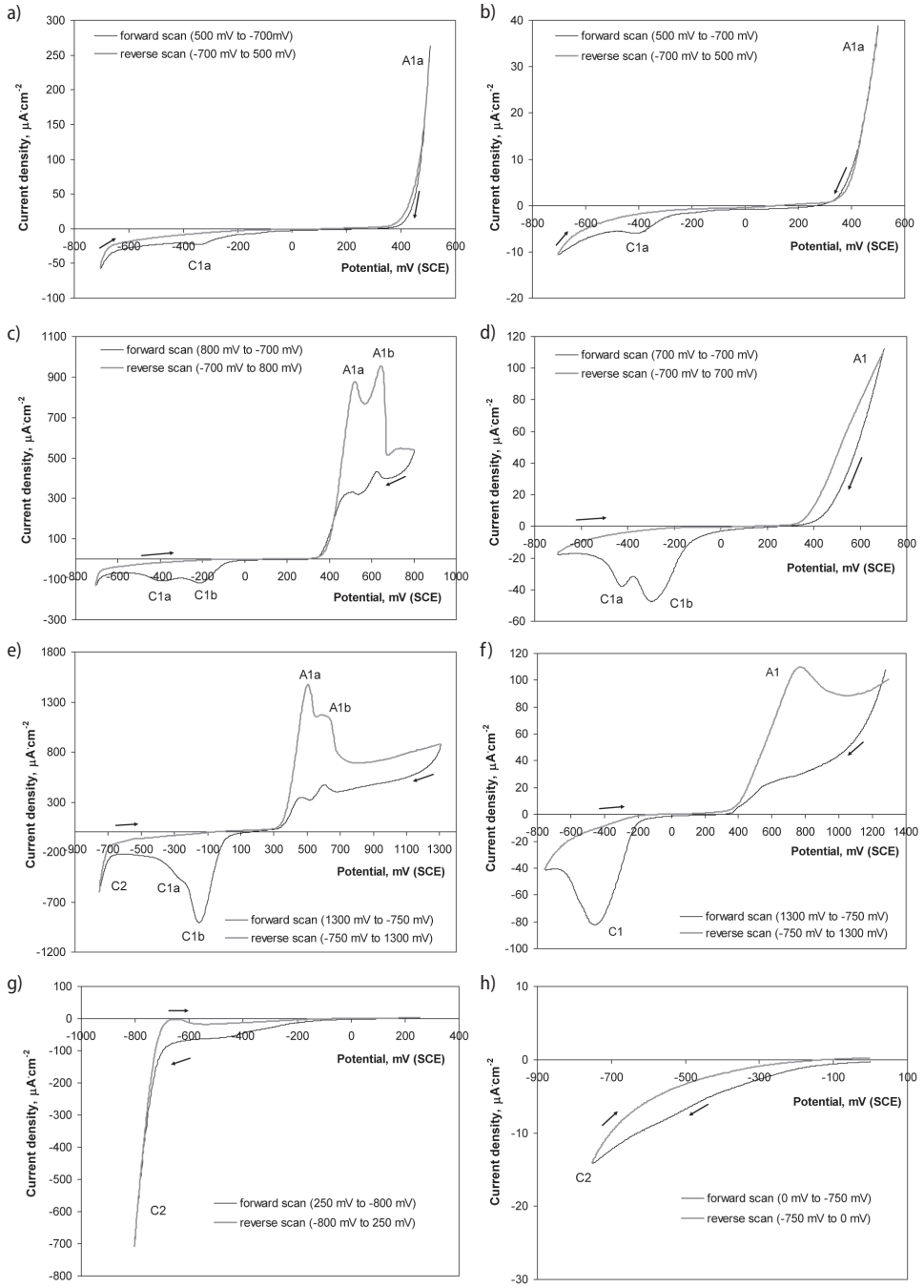

Fig. 2. Cyclic voltammograms for Te in HNO_3 solutions of pH 1.5 (left side: a, c, e, g) and 3.0 (right side: b, d, f, h). Scan rate: 10 mV/s; sweeps initiated towards negative potentials

Two anodic peaks (A1a, A1b) were recorded in the CV curves at pH of 1.5 and 2.0, independently on the direction of the initial sweep. Moreover, the coalescing anodic peaks were found in either forward or reverse scans, when the potential was cycled solely in the range from 100 (or 200) to 1300 mV (voltammograms not shown). No passivation effects were observed in these cases. It means that products of the anodic reactions (A1a, A1b) were formed directly from the bulk tellurium substrate and oxidation of products of another chemical or electrochemical reaction can not be taken into account as it was proposed by others [6, 10, 12]. Additionally, the presence of A1a and A1b peaks at pH 1.5 and 2.0 in the curves registered in both scanned directions (Fig. 1, Fig. 2 c, e) demonstrated that no tight layer of any solid product was formed on the tellurium surface. The increase in the solution pH suppressed the development of the anodic peaks indicating gradual covering of the electrode surface with an insulating layer of some solid product (Fig. 1, Fig. 2 d, f). It is worth also noting that the heights and areas of the cathodic peaks (C1) were smaller than for corresponding anodic peaks (A1) regardless of the forward sweep direction. Moreover, the cathodic peak C1a was smaller than C1b. It suggests that some soluble species were reduced at the C1a potential range indicating that products of tellurium oxidation can undergo some secondary processes.

To identify the products of the anodic oxidation of tellurium a set of potentiostatic measurements were performed. Tellurium was dissolved for 5 min at a constant potential of 510 mV in the solution of pH 1.5. The amount of tellurium present in the solution after electrolysis was compared with the amount of the charge flowed through the working electrode and number of electrons n participating in the elemental electrode reaction was calculated using the Faraday's law. It was found that n = 3.6 corresponding to four-electron anodic reaction of tellurium. According to the E-pH diagram [15] the expected soluble product of oxidation was $HTeO_2^+$. It is in accordance with the data reported commonly in the literature for the peak with the maximum at approx. 500 mV (SCE) [6, 10, 14]. Similar short potentiostatic measurements were not carried out in other conditions, since two concurrent processes can occur at a higher potential (e.g. 600 mV), whereas tellurium dissolution was inhibited at higher pH. Hence, it made impossible to obtain one soluble product of the anodic reaction.

Potentiostatic oxidation of tellurium for a prolonged period of time (45 min) led to the accumulation of solid products of the reaction on the electrode surface. Two kinds of products were observed by optical and scanning electron microscopes. Independently on the solution pH, oxidation of tellurium at 500 mV and 660 mV produced octahedral crystals, but at higher pH the electrode surface was increasingly covered with a white amorphous layer. Figure 3 shows the surface of tellurium after potentiostatic oxidation. EDS-SEM analysis of the crystals and white areas among the crystals showed the presence of tellurium and oxygen. It was difficult to determine definitely the formulas of the compounds due to simultaneous analysis of tellurium substrate. However, the O:Te atomic ratio in the crystals was 1.52 (39.7 ± 0.4 at% Te, 60.3 ± 0.8 at% O) suggesting the formation of TeO_2. Moreover, the shape of the crystals was

suitable for tetragonal system of TeO_2 [15]. The white product present on the electrode surface seemed to be porous and amorphous. It can correspond to tellurous acid H_2TeO_3 ($TeO_2 \cdot H_2O$) [15]. O:Te atomic ratios in the layer were approx. 0.73 (57.9 ± 1.0 at% Te, 42.2 ± 1.0 at% O).

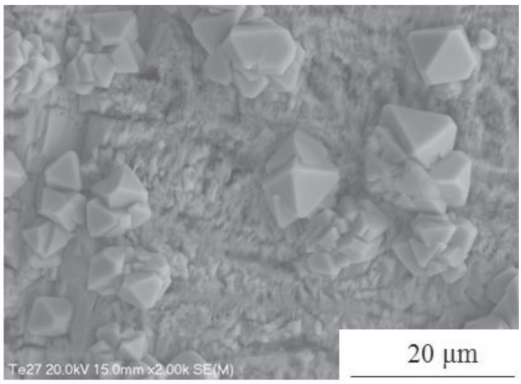

Fig. 3. Surface of tellurium after potentiostatic oxidation at 510 mV (SCE) in the solution of pH 1.5

An analysis of the solutions after potentiostatic oxidation was also carried out. It was found that the mass of tellurium dissolved from the electrode at each potential was less than the theoretical value calculated using the Faraday's law. It shows that tellurium oxidized initially to soluble species, but when the concentration of the species at the anode surface became high a formation of solid products occurred. This was confirmed by the current-time dependences shown in Figure 4. In the case of the potentiostatic oxidation with different applied potentials, there was always a dip in the current, then a rise to a steady state with the current intensity larger than the initial values. The minimum current intensity appeared after 50–250 s and it occurred earlier with higher potential and lower pH. Such a behavior was consistent with a mechanism of porous layer growth accepted commonly for anodic alumina formation as example [16]. According to this mechanism the linear current fall corresponds to the formation of a planar high-resistant film. After this film reaches a certain thickness, pores are nucleated over the surface. Tellurium oxide or tellurous acid film growth was accompanied by partial dissolution by the electrolyte. The rates of both processes were different, and the formation of the solids predominated over the secondary reaction. The solubility of the solid compounds was determined by solution pH. It was especially visible when the anodic process run at potential of 660 mV at pH 1.5. In this case fast oxidation of tellurium was accompanied by oscillations occurred after 1800 s of the electrolysis. It seems to be a resultant of two overlapping processes – formation of the oxide or acid layer under anodic polarization and secondary dissolution of the solid products to $HTeO_2^+$:

$$TeO_2 + H^+ \longrightarrow HTeO_2^+ \qquad (1)$$

$$H_2TeO_3 + H^+ \rightarrow HTeO_2^+ + H_2O \quad (2)$$

At higher solution pH lower currents were registered and oscillations were not observed due to less solubility of tellurium oxide or tellurous acid. It is in accordance with data of Issa and Awad [17], who reported that the solubility of TeO_2 in acidic solutions decreased from $4.2 \cdot 10^{-4}$ mol·dm^{-3} at pH 1.4 to a minimum (approx. $1 \cdot 10^{-5}$ mol·dm^{-3}) occurring at pH 3.8.

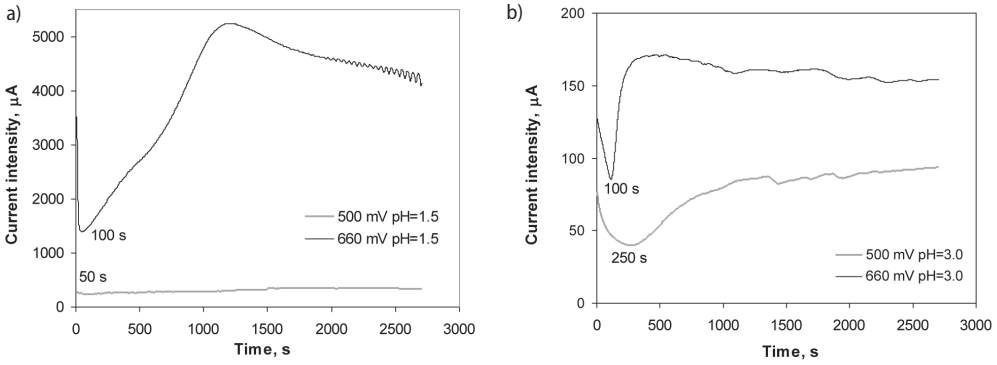

Fig. 4. Anodic current versus time curves for potentiostatic Te dissolution at potentials of 500 mV and 600 mV (SCE) in HNO_3 solutions of pH: a) 1.5; b) 3.0

Above considerations suggest that oxidation of tellurium at the potential of approx. 500 mV (A1a) is accompanied by the formation of soluble $HTeO_2^+$ ions as the intermediate product, but when the electrolyte at the anode surface becomes supersaturated in tellurium(IV) species, they convert into the final oxide product. At higher potentials, a thin film of tellurous acid can grow (A1b). It can be then reduced at the potential of approx. –200 mV (C1b). Both oxide and acid solid products chemically dissolve in the acidic electrolyte giving $HTeO_2^+$ species reduced then at the potential of approx. –400 mV (C1a). The rate of anodic tellurium dissolution directly to soluble species decreased with increased solution pH and solid products were favorably formed on the anode surface. Hindered dissolution of the solid products under electrolyte resulted in less pronounced the corresponding cathodic peak (C1a). It is consistent with results presented by Awad [13], who found that $HTeO_2^+$ and H_2TeO_3 were formed in the pH range of 0.8–1.8, whereas H_2TeO_3 was the only product of tellurium dissolution at higher pH. Similar conclusions were also presented by Jayasekera et al. [14]. They supposed that oxidation of tellurium above 1000 mV (SCE) in the pH range of 0–2.0 ($HClO_4$) gave sparingly soluble tellurous acid:

$$Te + 3H_2O \rightarrow H_2TeO_3 + 4H^+ + 4e \quad (3)$$

One cathodic peak at approx. –300 mV (SCE) was found by the authors [14] in the reverse scan, but depending on the switching anodic potential two different electrochemical reactions were ascribed to this cathodic peak. It was electrodeposition of elemental tellurium as a product of the reduction of $HTeO_2^+$ ions or H_2TeO_3 (process reversed to equation (3)). In contrast to the above, Barbier et al. [3] reported that anodic polarization of tellurium in H_2SO_4 solutions led to formation of TeO_2, which dissolved then as $HTeO_2^+$ ion and reduced to elemental tellurium at about –240 mV (SCE).

To confirm the nature of the anodic (A1a, A1b) and cathodic (C1a, C1b) peaks the CV curves were registered at various scan rates. The results for two pH values are presented in Figure 5. Typical effects were observed. Anodic and cathodic current densities increased with increased scan rate. All peaks moved apart and anodic and cathodic peaks drew along the potential axis towards positive and negative directions, respectively. It was obviously due to faster transport of the species to the electrode surface as well as the need of overpotential to drive the reactions. Two coalescing anodic peaks (A1a, A1b) evolved into one wide peak at pH 1.5 (Fig. 5a) and 2.0 (not shown) with the scan rate increased above 25 mV/s. Weak evident peak A1 at pH 2.5 (not shown) and 3.0 (Fig. 5b) disappeared and polarization curves were registered at the scan rates above 10 mV/s. One wide cathodic peak (C1) corresponding to the anodic ones (A1) was observed. Its area was much smaller than anodic for each sweep rate and pH value.

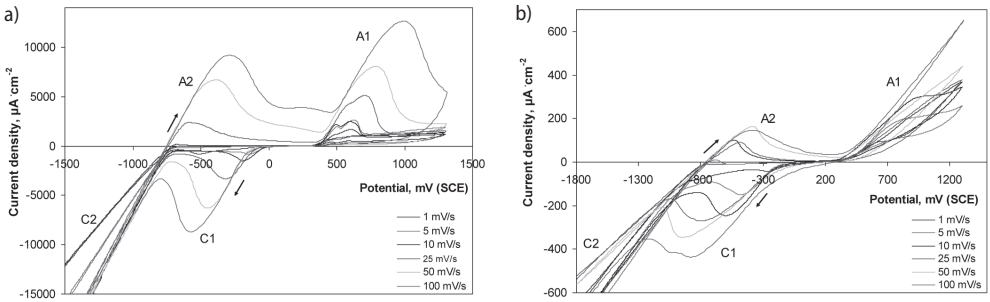

Fig. 5. Cyclic voltammograms registered at various scan rates for Te in HNO_3 solutions: a) pH = 1.5; b) pH = 3.0. Scan rate: starting potential: –1800 mV (SCE), sweeps commenced towards positive direction to 1300 mV

Some interesting features of the CV curves were found. The maximum of the peak C1 registered at pH 1.5 and 2.0 shifted gradually from approx. –150 mV for the scan rate of 5 mV/s to approx. –600 mV for 100 mV/s. However, for the slowest scan rate (1 mV/s) a small cathodic peak was observed at the potential of –500 mV. The latter was understandable for reduction of the soluble Te(IV) species present in the electrolyte. It can confirm that the peak C1a at pH 1.5 and 2.0 corresponds to the reduction of $HTeO_2^+$ ions formed (directly in the electrochemical reaction or as a product of the

secondary process) in the former anodic range, where two coalescing peaks were developed. At the low scan rate longer time was needed to sweep the potential range. It was sufficient to partial dissolution of oxide or acid film from the tellurium surface and to deliver a part of $HTeO_2^+$ ions from the electrode vicinity, hence a higher overpotential was necessary for the cathodic process (C1a). At higher sweep rates formation of sparingly soluble products was more favored due to faster saturation of the electrolyte at the electrode surface with the Te(IV) species. It brought the cathodic peak at the potential of –200 mV (C1b) in the reverse scan and its shift towards negative direction with an increased scan rate. At pH 2.5 and 3.0 only one cathodic peak was registered for all sweep rates. It was attributed directly as the peak C1b, since it moved from –200 mV to the negative direction with the scan rate changed from 1 mV/s to 100 mV/s.

3.3. Cathodic polarization

General cyclic voltammograms registered in the entire studied potential range (Fig. 1) showed that the formation of the anodic peak A2 was directly correlated with previous cathodic currents flowed in the potential range C2. Figure 6 shows the voltammetric behavior of tellurium at low electrode potentials. The CV curves were registered from –200 mV to various switching potentials with the negative-going forward scans. It was observed that cathodic the current increased rapidly below –700 mV. The point where the potential sweep was reversed was of a great importance to the presence and height of the anodic peak A2 in the backward scan. If the switching potential did not exceed –700 mV in the solution with pH 1.5 only cathodic currents were recorded. The range of solely cathodic currents was extended up to –900 mV with pH increased to 3.0. The anodic peak A2 appeared in the backward scan for the reversal potentials less than the given values. The height of the peak A2 was dependent on the final potential of the forward step and solution pH alike. In the most acidic solution the anodic peak arose with the change of the switching potential from –800 to –900 mV, but it disappeared gradually with further decrease in the reversal potential. Such a tendency was not observed at higher pH values, where an increase in the peak area with more negative reversal potentials was observed. It was accompanied by the shift of the peaks towards more positive values (in the range from –680 to –610 mV), whereas the peak maximum at pH 1.5 remained unchanged (–660 ± 5 mV).

Faster scan rates enhanced the growth of the peak A2, independently on the solution pH (Fig. 5), but no anodic peak was detected for the slowest rate (1 mV/s). It was understandable if soluble species were considered as a reaction substrate. At low sweep rate the mass transport by diffusion or convection became important. In such a case, concentration of the soluble species produced in the forward cathodic scan decreased at the electrode surface before subsequent backward anodic sweep. At higher sweep rates, the time necessary to scan a given potential range was much shorter and it was enough to detect the species in the electrochemical process.

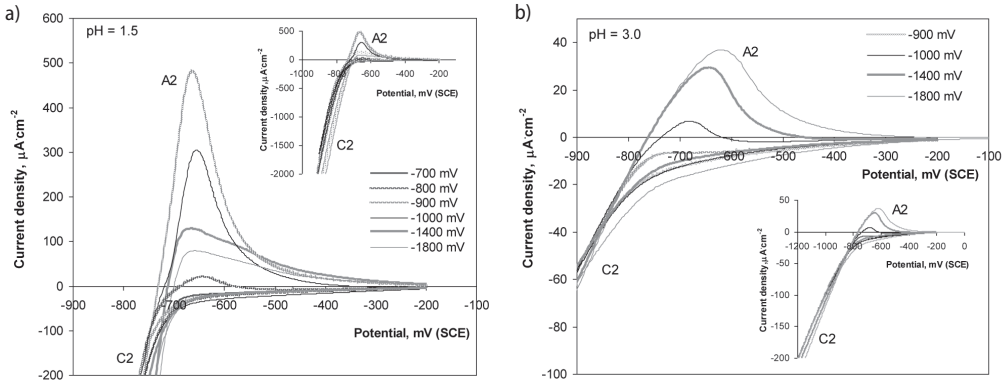

Fig. 6. Cyclic voltammograms for Te in HNO3 solutions: a) pH = 1.5, b) pH = 3.0. Scan rate: 10 mV/s; starting potential: –200 mV (SCE), sweeps commenced towards negative direction to various switching potentials

The extending of the sweeping range towards more negative potentials (forward scan) caused changes on the electrode surface. It became dark at the potential of –1000 mV, but below –1100 mV a black slime run down into solution. The characteristic odor of hydrogen telluride H_2Te was also noticed during cathodic polarization, while below –1300 mV bubbles of a gas on the electrode surface were visible. Moreover, a silvery film on the electrolyte surface in the electrode vicinity was formed already during the forward step.

An attempt of quantitative analysis of the black slime was made. The potentiostatic measurements at the potential of –1300 mV (pH 1.5 and 3.0) were performed. The slime was very fine grained and dissolved slowly in the electrolyte, but it was possible to accumulate the powder in the amount sufficient for the chemical analysis. Such degradation of the tellurium electrode was observed earlier by others [3], but since now no identification of the compound was reported.

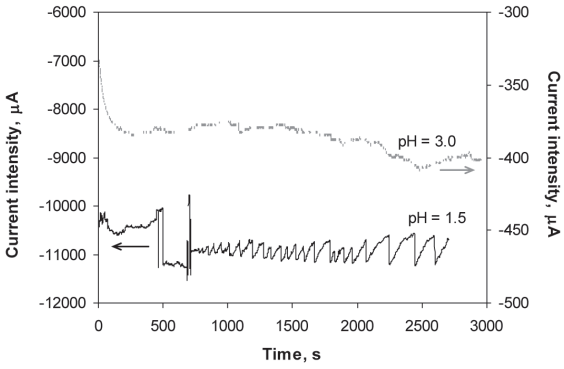

Fig. 7. Current-time curves registered during potentiostatic cathodic dissolution of tellurium at –1300 mV (SCE) in HNO_3 solutions of pH 1.5 and 3.0

Figure 7 shows current-time curves registered during potentiostatic cathodic dissolution of tellurium. Oscillations of the current occurring at the electrode were observed, especially in the most acidic solution. This periodic phenomenon appeared after some time of the electrolysis. It could be explained by removal of the slime from the electrode surface by H_2Te or H_2 evolved at the cathode. This is quite different from the mechanism of current oscillations generated with anodic polarization (Fig. 4), which involved precipitation and secondary dissolution steps.

Linear voltammetric curves were recorded for tellurium cathodes in HNO_3 solutions with pH 1.5 and 3.0 and presented in Figure 8. Three linear regions (a–c) indicated that various cathodic reactions could occur below –200 mV. The first section (a) was in the potential range from –200 mV to –650 mV for pH 1.5 and to –850 mV for pH 3.0. The slope of this section was high (171–650 mV/dec) and corresponded probably to the double layer charging. The second linear portion of the polarization curve (b) was in the potential range from –700 to –810 mV for pH 1.5, and it shifted towards more negative potentials with increased pH (from –900 to –1100 mV for pH 3.0). It represented the evolution of H_2Te. The slope of this section was approx. 90 ± 1 mV/dec at pH 1.5 and 2.0 and was close to the value 92 mV/dec determined in acidic chloride solution for potentials below –800 mV, which was ascribed to H_2Te evolution [1, 2]. The third linear section of the curve (c) was reached at much lower potentials (below c.a. –1150 mV for pH 1.5–2.5 and below c.a. –1400 mV for pH 3.0). It corresponded to the formation of a black slime on the tellurium cathode due to the intense coevolution of H_2Te. The layer of the powder covered the cathode surface and increased the polarization considerably (the slopes reached approx. 1500 mV/dec).

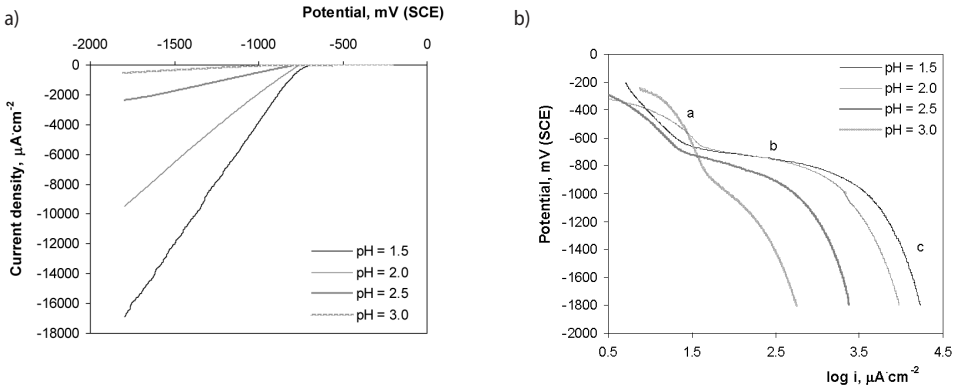

Fig. 8. Linear voltammetric curves recorded for tellurium cathodes in HNO_3 solutions with various pH: a) polarization curves; b) Tafel plot. Starting potential: –200 mV (SCE), sweep rate 10 mV/s

The changes at the cathode surface affected the anodic peak in the reverse scan. It was especially visible for pH 1.5. Decrease the final potential (less than –1000 mV) during forward scan caused more intensive production of the slime and gradual reduction of

the peak A2 in the backward scan (Fig. 6a). It was obvious that the anodic peak A2 was due to the oxidation of H_2Te evolved previously in the C2 potential range [2–4, 14]. Hence, the gradual decrease in the anodic peak area could be due to the partial consumption of hydrogen telluride in the secondary reaction with the slime as a final product. It seems that H_2Te evolved in the electrochemical reaction can dissolve in the aqueous solution and decompose to elemental tellurium. It occurs immediately even at low concentrations of oxygen dissolved in the electrolyte [18]:

$$H_2Te_{(aq)} + \tfrac{1}{2}O_2 \rightarrow Te + H_2O \tag{4}$$

Formation of a bright, silvery film drifting on the electrolyte surface at the electrode surface was also understandable due to the decomposition of gaseous H_2Te electrochemically generated in acidic solution [2, 18] to tellurium (confirmed by XRD analysis, results not shown) and hydrogen:

$$H_2Te_{(g)} \rightarrow Te + H_2 \tag{5}$$

Gaseous hydrogen telluride as an endothermic compound ($\Delta H° = 100$ kJ/mol) can decompose slowly into elemental tellurium already at 273 K [18]. This process was applied by Engelhard et al. [19] as a simple method of tellurium thin film deposition on polyethylene substrate.

Degradation of tellurium electrode during cathodic polarization was observed by Barbier et al. [3], who supposed that tellurium powder precipitated in the solution. Deposition of tellurium at the potentials below –600 mV (SCE) was also reported by other authors [8–11]. They considered secondary reactions between H_2Te and $HTeO_2^+$. However, such an approach can not be correct in the presented study due to the absence of $HTeO_2^+$ ions in the electrolyte (a lack of the cathodic peaks C1 in the CV forward scans in Figure 6).

3.4. Summary

A comparison of the experimental data with the potentials calculated according to the thermodynamic data (Tab. 1) as well as additional cyclic voltammograms registered in nitrate solutions saturated with TeO_2 (Fig. 9) allowed confirming or excluding correctness of the argumentation. Obviously, it should keep in mind that the peak potentials determined experimentally can not reflect strictly equilibrium values due to various overpotentials necessary to the course of reactions, particularly on different substrates.

Equilibrium potentials calculated for Te/H_2TeO_3, $Te/HTeO_2^+$ and Te/TeO_2 shows that with the increase in the electrode potential above 100 mV formation of soluble Te(IV) species from elemental tellurium followed by oxidation to solids is thermodynamically

expected. The difference in the maximum potentials A1a and A1b at pH 1.5 was approx. 150 mV and it seems to be in accordance with the difference of the equilibrium potentials for Te/H_2TeO_3 and Te/$HTeO_2^+$ electrodes (110 mV). At higher pH the calculated potentials of Te/$HTeO_2^+$ and Te/TeO_2 electrodes are close together and formation of tellurium oxide due to its less solubility should be promoted.

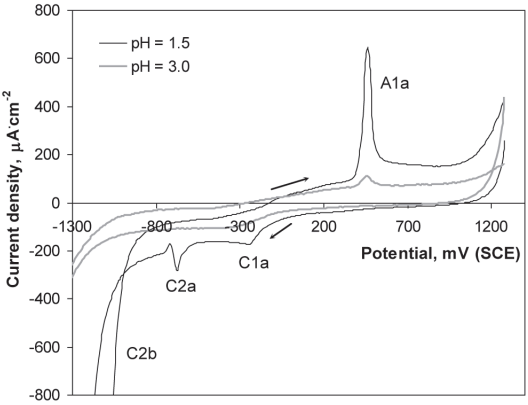

Fig. 9. Cyclic voltammograms registered in nitrate solutions saturated with TeO_2 on glassy carbon electrode

Table 1. Electrode potentials (298 K)

Electrode reaction	Standard electrode potential*, mV		Equilibrium potential**, mV (SCE)	
	vs NHE	vs SCE	pH = 1.5	pH = 3.0
$Te + 3H_2O \rightarrow H_2TeO_3 + 4H^+ + 4e$	614	373	284	196
$Te + 2H_2O \rightarrow HTeO_2^+ + 3H^+ + 4e$	550	309	169	102
$Te + 2H_2O \rightarrow TeO_2 + 4H^+ + 4e$	540	299	210	122
$2H_2Te_{aq} \rightarrow Te_2^{2-} + 4H^+ + 2e$	–142	–383	–413	–590
$H_2Te_{aq} \rightarrow Te + 2H^+ + 2e$	–471	–712	–653	–742
$Te_2^{2-} \rightarrow 2Te + 2e$	–800	–1041	–893	–893
$H_2 \rightarrow 2H^+ + 2e$	0	–241	–330	–418

* Standard electrode potentials were calculated according to standard free energies presented by Mc'Phail [20], except for $HTeO_2^+$ [15]

** Equilibrium potentials were calculated for 10^{-5} M tellurium soluble species

Formation of $HTeO_2^+$ ions from elemental tellurium at the potential of approx. 500 mV was confirmed by voltammograms registered on glassy carbon substrate in Te(IV) nitrate solutions (Fig. 9). Anodic peak A1a appeared at the potential of approx. 460 mV and

corresponded to the dissolution of formerly deposited tellurium at the potential of approx. –300 mV (peak C1a in Figure 9). No peak labeled as A1b in Figure 1 was found in voltammograms for glassy carbon electrode. It was obvious, since only a limited amount of tellurium was deposited in the negative-going sweep.

The experimental range of the potentials, where bulk tellurium was reduced to H_2Te followed by H_2Te oxidation covers also the equilibrium potential for Te/H_2Te electrode. Voltammograms determined in the tellurium(IV) acidic electrolyte showed a distinct peak C2a at –680 mV corresponding to the H_2Te evolution followed by a further increase in the cathodic current C2b due to the reduction of hydrogen ions. No anodic peak (A2) was found in the reverse scan, since hydrogen evolution seemed to be a main former reaction.

According to the thermodynamic calculations reduction of tellurium to Te_2^{2-} species can occur at potentials below c.a. –900 mV (SCE). However, it was omitted, since no additional anodic peak in the potential range from –400 to –600 mV (depending on pH) representing Te_2^{2-} to H_2Te oxidation was observed.

The products of the electrochemical processes can convert into other compounds. It can be done under an electrolyte (dissolution of H_2TeO_3 and TeO_2) or in another spontaneous processes. The latter is represented by the formation of tellurium from H_2Te. It was supposed that the black powder (slime) or the bright film of elemental tellurium precipitated in two different secondary chemical reactions.

4. Conclusions

The electrochemistry of tellurium was studied in acidic nitrate solutions with pH 1.5–3.0. It was found that two products were formed at potentials above 300 mV (SCE): soluble $HTeO_2^+$ and sparingly soluble H_2TeO_3, but the former seemed to be an intermediate product for TeO_2 precipitation on the electrode surface. The formation of the solid products was almost undisturbed and no passivation was observed, since porous layers were created on the anode surface. H_2TeO_3 and TeO_2 can dissolve to $HTeO_2^+$ under acidic electrolyte, but this process was hindered by pH increase from 1.5 to 3.0. Cathodic polarization of tellurium electrode below –800 mV was accompanied by H_2Te evolution, which was then oxidized at the potentials approx. –700 mV (SCE). H_2Te generated in the electrochemical reaction decomposed partially to elemental tellurium forming black powdery precipitates in the bulk of the solution and a bright film drifting on the electrolyte surface.

Acknowledgements

This research study was financed from funds of Ministry of Science and Higher Education as a development project No. N R07 0017 04.

References

[1] Bard A.J. (ed.): *Encyclopedia of electrochemistry of the elements*. Vol. 4. Marcel Dekker, New York, 1975, 393–443

[2] *Gmelin handbook of inorganic chemistry*. Te. Supplement 42 (1983), 224–281

[3] Barbier M.-J., de Becdelievre A.-M,. de Becdelievre J.: *Electrochemical study of tellurium oxido-reduction in aqueous solutions*. Journal Electroanalytical Chemistry, 94 (1978), 47–57

[4] Rosamilia J.M., Miller B.: *Voltammetric studies of tellurium film and hydrogen telluride formation in acidic tellurite solution*. Journal of Electroanalytical Chemistry, 215 (1986), 261–271

[5] Mori E., Baker C.K., Reynolds J.R., Rajeshwar K.: *Aqueous electrochemistry of tellurium at glassy carbon and gold. A combined voltammetry – oscillating quartz crystal microgravimetry study*. Journal of Electroanalytical Chemistry, 252 (1988), 441–451

[6] Traore M., Modolo R., Vittori O.: *Electrochemical behaviour of tellurium and silver telluride at rotating glassy carbon electrode*. Electrochimica Acta, 33, 7 (1988), 991–996

[7] Gregory B.W, Norton M.L., Stickney J.L.: *Thin-layer electrochemical studies of the underpotential deposition of cadmium and tellurium on polycrystalline Au, Pt and Cu* electrodes. Journal of Electroanalytical Chemistry, 293 (1990), 85–101

[8] Dennison S., Webster S.: *An electrochemical and optical microscopic study of the reduction of* $HTeO_2^+$ *in aqueous acid solution*. Journal of Electroanalytical Chemistry, 314 (1991), 207–222

[9] Montiel-Santillán T., Solorza O., Sánchez H.: *Electrochemical research on tellurium deposition from acid sulfate medium*. Journal of Solid State Electrochemistry, 6 (2002), 433–442

[10] Han D.-H., Choi S.-J., Park S.-M.: *Electrochemical Preparation of Zinc Telluride Films on Gold Electrodes*. Journal of Electrochemical Society, 150 (5) (2003), C342–C346

[11] Martin-Gonzalez M.S., Prieto A.L., Gronsky R., Sands T., Stacy A.M.: *Insights into the Electrodeposition of* Bi_2Te_3. Journal of Electrochemical Society, 149 (11) (2002), C546–C554

[12] Wen S., Corderman R.R., Seker F., Zhang A.-P., Denault L., Blohm M.L.: *Kinetics and Initial Stages of Bismuth Telluride Electrodeposition*. Journal of Electrochemical Society, 153, 9 (2006), C595–C602

[13] Awad S.A.: *Anodic dissolution of tellurium in acid solutions*. Electrochimica Acta, 12 (1968), 925–936

[14] Jayasekera S., Ritchie I.M., Avraamides J.: *A Cyclic Voltammetric Study of the Dissolution of Tellurium*. Australian Journal of Chemistry, 47, 10 (1994), 1953–1965

[15] Pourbaix M.: *Atlas of Electrochemical Equilibria in Aqueus Solutions*. Pergamon, New York, 1966

[16] Bockris J. O'M., White R.E., Conwey B.E. (eds): *Modern aspects of electrochemistry*. No. 20. Plenum Press, New York, London

[17] Issa I.M., Awad S.A.: *The Amphoteric Properties of' Tellurium Dioxide*. Journal of Physical Chemistry, 58 (1954), 948–951

[18] Bielański A.: *Podstawy chemii organicznej* [Fundamentals of inorganic chemistry]. Wydawnictwo Naukowe PWN, Warszawa, 1994 [in Polish]

[19] Engelhard T., Jones E.D., Viney I., Mastai Y., Hodes G.: *Deposition of tellurium films by decomposition of electrochemically-generated H2Te: application to radiative cooling devices*. Thin Solid Films, 370 (2000), 101–105

[20] McPhail D.C.: *Thermodynamic properties of aqueous tellurium species between 25 and 350°C*. Geochimica Cosmica Acta, 59, 5 (1995), 851–866